



**AUTHOR(S):**

**TITLE:**

**YEAR:**

**Publisher citation:**

**OpenAIR citation:**

**Publisher copyright statement:**

This is the \_\_\_\_\_ version of an article originally published by \_\_\_\_\_  
in \_\_\_\_\_  
(ISSN \_\_\_\_\_; eISSN \_\_\_\_\_).

**OpenAIR takedown statement:**

Section 6 of the "Repository policy for OpenAIR @ RGU" (available from <http://www.rgu.ac.uk/staff-and-current-students/library/library-policies/repository-policies>) provides guidance on the criteria under which RGU will consider withdrawing material from OpenAIR. If you believe that this item is subject to any of these criteria, or for any other reason should not be held on OpenAIR, then please contact [openair-help@rgu.ac.uk](mailto:openair-help@rgu.ac.uk) with the details of the item and the nature of your complaint.

This publication is distributed under a CC \_\_\_\_\_ license.

\_\_\_\_\_



2nd International Conference on Structural Integrity, ICSI 2017, 4-7 September 2017, Funchal, Madeira, Portugal

## Mixed-mode fracture characteristics of metal-to-metal adhesively bonded joints: experimental and simulation methods

M G Droubi\*, J McAfee, R C Horne, S Walker, C Klaassen, A Crawford, A K Prathuru and N H Faisal\*

*School of Engineering, Robert Gordon University, Garthdee Road, Aberdeen, AB10 7GJ, UK*

---

### Abstract

Fracture behavior of adhesively bonded joints subjected to mixed-mode (i.e. mode I+II) loading conditions is of importance in many industrial applications. This research therefore aims to characterise the failure behaviour of metal-to-metal (i.e. both aluminium adherends) adhesive joints using the mixed mode bending test (MMB), adapted from ASTM D6671/D6671M standard, along with instrumentation using acoustic emission (AE) sensor. Twenty-four adhesively bonded specimens were prepared using two types of adhesive bond materials (acrylic, cyanoacrylate) with two different bonded area 65% and 100%. To understand the effect of mixed-mode loading conditions on the failure behavior, two different mixity ratios were achieved through the design of the MMB test fixture and tested for each bonded joint. The AE results during mechanical testing shows that the time domain signals were spread over the loading phase with distinct features for different mixity ratios. They successfully identified the moment of adhesive fracture during every test. Also, the fracture behavior of the bonded joints was simulated using virtual crack closure technique (VCCT) method using finite element method to understand the loading dynamics in specimen when considering a combination of various design parameters. In addition, an analytical method (e.g. corrected beam theory or CBT) was used to determine strain energy release rates of each specimen. The results show that both the brittle and ductile specimens exhibited higher energy release rates when mode II proportion of loading was increased during the crack initiation phase. The proposed measurement can be useful to assess the overall structural health of bonded systems.

© 2017 The Authors. Published by Elsevier B.V.

Peer-review under responsibility of the Scientific Committee of ICSI 2017

*Keywords:* mixed-mode fracture; adhesively bonded joints; acoustic Emission

---

\* Corresponding author. Tel.: +44(0)1224-26-2336.

*E-mail address:* [m.g.droubi@rgu.ac.uk](mailto:m.g.droubi@rgu.ac.uk); [n.h.faisal@rgu.ac.uk](mailto:n.h.faisal@rgu.ac.uk);

## 1. Introduction

The joining of two or more components is the main objective of fabrication and has been historically present throughout several engineering applications such as marine, automobile, aerospace and construction. This allows for structures or physical systems to perform to their operational requirements, transferring forces from one surface to another, whilst exchanging overall attributes such as weight, size and strength specific to their purpose. The adoption of adhesive bonding is mainly due to the advantages that it provides over mechanical fixing techniques (i.e., welding, screws and bolts) including but not limited to: reductions in weight, the variety of materials that can be bonded, a uniform stress distribution on the load, strong cohesive properties and a resistance to corrosion. From literature, three main crack types (failure modes) exist: mode I, dictated by normal opening forces, and modes II and III, defined by in-plane and out of plane shear sliding forces respectively (Choupani, 2008).

To further develop the performance and safety of adhesively bonded joints, a greater understanding of their behaviour in relation to these three modes must be acquired. Adhesive bonds are specifically subject (but not limited) to two major types of failure: adhesion, a failure at the bond interface, and cohesion, caused by failure within the adhesive material itself. Although many manufacturers are aware of these behavioral characteristics and their common causes, there is much less of an understanding of the combinational effects. Within the aerospace industry alone, difficulty has been reported in understanding the mechanism of transition, from a strong bond displaying cohesive failure to a weak bond exhibiting adhesion failure (Davis and McGregor, 2010). With many inspection techniques occurring after a major incident, this transition is overlooked, incorrect conclusions are drawn and issues are not addressed. Therefore, it is imperative to investigate this subject thoroughly to avoid potential disaster.

Although many monitoring procedures used to predict failure within adhesive joints, such as eddy current, neutron radiography and infrared spectroscopy, only a small number of these procedures have proven to be effective in predicting failure. Ultrasonic testing is by far the most commonly used method, allowing for sub-millimetre detection of failed or misdirected adhesive. However, the ultrasound must be coupled with water and moved over every area of the component to be tested, which can be time-consuming (especially over large areas) (Vine, 1999). Acoustic emission (AE) technique can be used to detect transient elastic waves emitted by a growing fracture or stress level within the material (Sachse and Kim, 1987). As this is the only non-destructive testing method that utilises energy released from the material under examination, sensors can receive signals originating from various locations, reducing direct contact area and time taken to test. The specific ability to monitor components during the loading lifespan allows for a greater understanding of the initiation and growth of cracks. Because of this, AE can be employed in the identification of failure at extremely early stages, preventing catastrophic structural damage. Dzenis and Saunders (2002) have attempted to characterise AE signals from various fracture mechanisms under mode I, mode II and mixed-mode fracture of adhesively bonded joints, using computational pattern recognition analysis. Using two wideband sensors placed on either side of the crack tip, a clear separation of the pure mode was observed, while mixed-mode signals were found to be like those of mode II.

In this study, the effects of varying adhesive type (ductile or brittle), quality of bond (adhesive contact area) and mode-mixity (i.e. ratio of mode I to mode II failure) of the specimens were investigated. To inflict mixed-mode loading conditions, a purpose built and standardised mixed-mode bending (MMB) test rig was developed. Also, the behaviour of adhesively bonded joints under mixed-mode loading was examined, incorporating finite element (FE) analysis, analytical calculations and an experimental MMB test procedure.

## 2. Experimental procedure

### 2.1. Specimen preparation

Each specimen comprised of two identical aluminium-alloy 6082 bars (Fig. 1a), to the specified dimension of 200 mm x 25 mm x 6 mm. Two 3.6 mm countersunk holes were drilled through one side of the bars to accommodate two countersunk head M3 screws. Hinges were screwed on to the specimens and connected to the hinge clamps of the MMB fixture. To remove dirt and contaminants, each specimen was wiped down thoroughly with acetone from an applicator bottle; after which, each section was sprayed with Loctite® SF 7063™ aerosol multi-purpose cleaner and wiped down to further remove any impurities. After allowing the specimens to air-dry, Loctite® 7649™ adhesive

activator was applied across the bonding surface of each section to improve adhesion and reduce the curing time. To ensure that there was no bonding at the designated pre-crack, Rocol® Dry Polytetrafluoroethylene (PTFE) spray was generously applied to a 60-mm section at the hinge end of each specimen. PTFE was again used to control the bond strength of any specimens that were to have 65% bonded area, this involved placing a 3D-printed template over the activated side of each specimen and spraying evenly (Prathuru et al. (2016)). For fully bonded specimens, PTFE was applied only at the pre-crack. The specimens were left to air-dry until any excess PTFE had evaporated and the residue was visible. At this stage adhesive (Loctite® AA326™ ductile adhesive or Loctite® EA3430™ brittle adhesive) was applied generously to the treated area of one specimen. The adhesive was then spread evenly across the specimen using a spreading stick (cleaned with acetone) to ensure an even distribution. The two treated adherends were then carefully placed together, ensuring that both were correctly aligned, and a wooden section and 10 N weight were placed on top to ensure a uniformly distributed load while the adhesive cured (maintaining a uniform bond thickness under the applied weight, defined as no-gap condition by Prathuru et al. (2016)). Specimens prepared with ductile adhesive were left to cure for four days where specimens prepared with brittle adhesive were left to cure for one day.

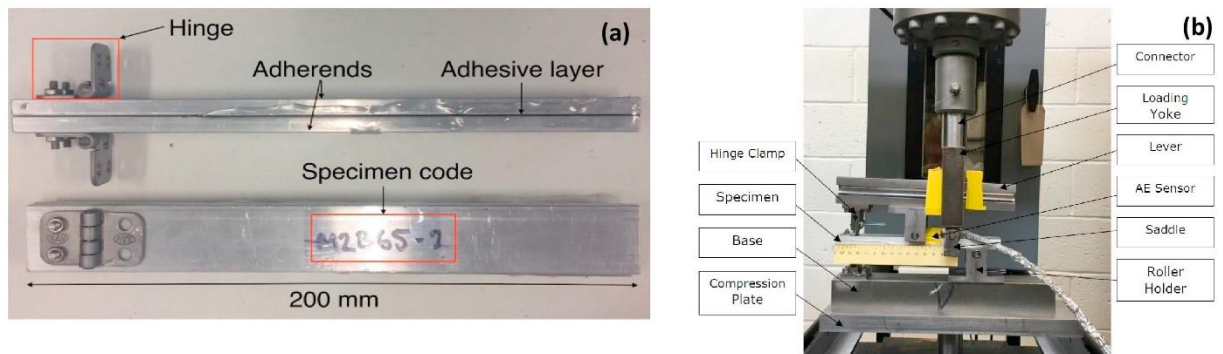


Fig. 1. (a) adhesively bonded specimen with hinges; (b) Mixed-mode bending MMB experimental set-up with specimen and AE sensor.

## 2.2. Instrumented mixed mode bending test

Instrumented mixed mode bending (MMB) setup, shown in Fig. 1b, which was manufactured, in accordance with ASTM D6671/D6671M (2013), for this test includes a rig adaptor (jig) that can be inserted into the tensile testing machine (Instron® Model 3382, High Wycombe, UK) to be pulled apart at a user-defined rate through the BlueHill 3.0 software. To ensure that the fixture was rigidly fixed and there was no free movement, a compression plate was designed and fabricated to fix the base of the testing machine while still allowing for variations of the lever arm length to be made. This also ensured the desired loading points were aligned correctly with the top and bottom loading cells. Top and bottom connectors were also designed and fabricated so that the fixture was connected to the Instron machine.

The bonded specimens were secured to the fixture using hinges fixed with countersunk screws, to allow clearance during adhesive bonding. This enabled the rotation of the lever relative to the horizontal axis, to provide the bending force required. The hinges were then screwed to the hinge clamps. All bolts used were tightly fastened prior to loading. Holes specifically drilled in the top of the lever and bottom of the base allowed for the fixture to be assembled to achieve the lever arm lengths which gave the two mixed-mode ratios being tested. A displacement rate of 2 mm/min was chosen for all test runs while load vs. displacement was recorded at 100 data points per second. To ensure a good repeatability of results, each test was repeated three times. To determine the fracture toughness of each specimen, constituent strain energy release rates,  $G_I$  and  $G_{II}$  were calculated.

A differential AE sensor with frequency range of 100 kHz to 1000 kHz (Model: Micro-80D, Physical Acoustics Ltd, Cambridge, UK) with 340 kHz resonance frequency was used throughout the investigation. The AE sensor was held in place using electrical tape 120 mm from the pre-crack edge and located behind the mid-roller (Fig. 1b). Silicone grease was applied to the sensor before attaching to the specimen surface, while the sensor was connected to a pre-amplifier and then to signal conditioning unit and data acquisition card. The data was recorded continuously for the entire test within newly developed LabVIEW code while AE signal acquisition was carried out at 2 MHz.

Two mode mixities (I+II) were tested through the design of the MMB test fixture. The change in mode-mixity was achieved by varying the lever arm length, which could be unscrewed and changed easily. The mixed-mode ratios tested were 2:1 and 1:2, so that the mode I and mode II energy release rate contributions could be assessed. Brittle and ductile adhesives were used to analyse how the adhesive’s properties affect its bonding capabilities under mixed-mode loading. Finally, the bond strength was varied by changing the percentage of surface area bonded. The adhesive joints were either partially bonded (65% bond area) or fully bonded (100% bond area) together.

Multiple methods were utilised to analyse the fracture properties of adhesively bonded joints undergoing mixed-mode (I+II) failure. The information gathered from the experimental MMB test outlined the loading response and exemplified the integrity of the adhesive bond, with a focus on the linear elastic region. From this, the mechanical events were interpreted and associated with post-test specimen profiles and video captured images. Features such as initial fracture type, stick-slip and the nature of debonding were discussed. To efficiently present each individual specimen type during testing and the presentation of results, a systematic sample coding system was required. Table 1 shows the coding key used to represent each feature of the specimen being tested. Mode-mixity 1 (M1) represents the configuration of the fixture that gave a ratio of 2:1 for  $G_I/G_{II}$ . Mode-mixity 2 (M2) represents the configuration of the fixture that gave a ratio of 1:2 for  $G_I/G_{II}$ .

Table 1. Specimen coding

Configuration	Code	Configuration	Code	Configuration	Code
Mode-mixity 1	M1	Brittle adhesive	B	65% bonded	65
Mode-mixity 2	M2	Ductile adhesive	D	100% bonded	100

2.3. Finite element analysis

As per the MMB scheme shown in Fig. 2a, a two-dimensional finite element modelling of the MMB specimens was carried out using ANSYS Workbench (Fig. 2b). A 60-mm pre-crack was simulated by splitting the lines of the adherend geometry in contact with each other, so that different behaviours could be modelled along the interface. To simulate the interface between the adhesive and adherends, VCCT was applied at the interface. The material properties used for the adherends were linear isotropic. The linear isotropic behaviour of aluminium-alloy 6082 was derived from Young’s modulus and Poisson’s ratio, with input values of 70 GPa and 0.3, respectively. As can be seen in Fig. 2b, displacements were applied at nodes at the upper left side and centre of the upper adherend to simulate the loading conditions. The values used were relative to the mode-mixity being tested. Fixed supports were applied to the two nodes at the bottom corners of the lower adherends.

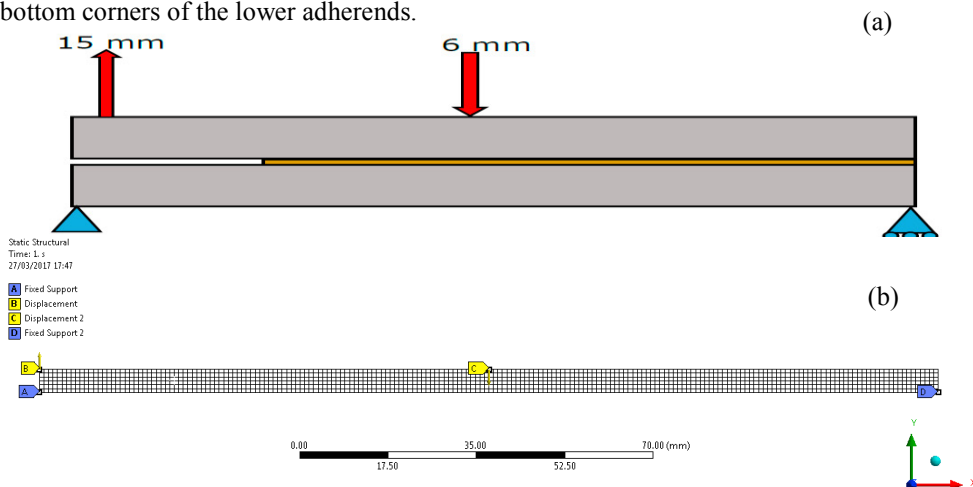


Fig. 2. (a) schematic of mixed-mode (I+II) bending test; (b) loading and boundary conditions in mixed-mode (I+II) bending FE model.

### 3. Results and discussion

#### 3.1. Instrumented mixed mode bending test

Figure 3 shows the loading graphs for mode-mixity 1 (M1) using ductile adhesive and fully bonded specimen. As can be seen, the loading graphs were divided into three stages: a pre-loading stage (1) of the MMB apparatus where the loading yoke was lowered onto the saddle bearings resulting in compression throughout the fixture to eradicate gaps, a linear elastic deformation stage (2) of the adhesive and a final stage (3) of adhesive layer debonding, most commonly experienced at the upper adherend interface due to the bending forces exerted by the lever. To prevent plastic deformation of the hinges, the test was stopped at a deflection of 5 mm. It can be noted here that in the post-test specimen profiles there was either an initial cohesive failure, interfacial failure or combination of the two. As the adhesive was applied with the applicator gun and spread evenly, the running of adhesive onto the pre-crack area was difficult to control. As a result of this, the adhesive interface between the materials was very weak on those areas. Once the load was applied, the bending force present in the top adherend debonded the overhanging adhesive. Then, once the critical energy release rate was met, cohesive failure occurred as signified in the loading graphs. This was indicative of sufficient bond preparation; however, an adhesive failure at the upper metal-adhesive interface also occurred in many of the samples.

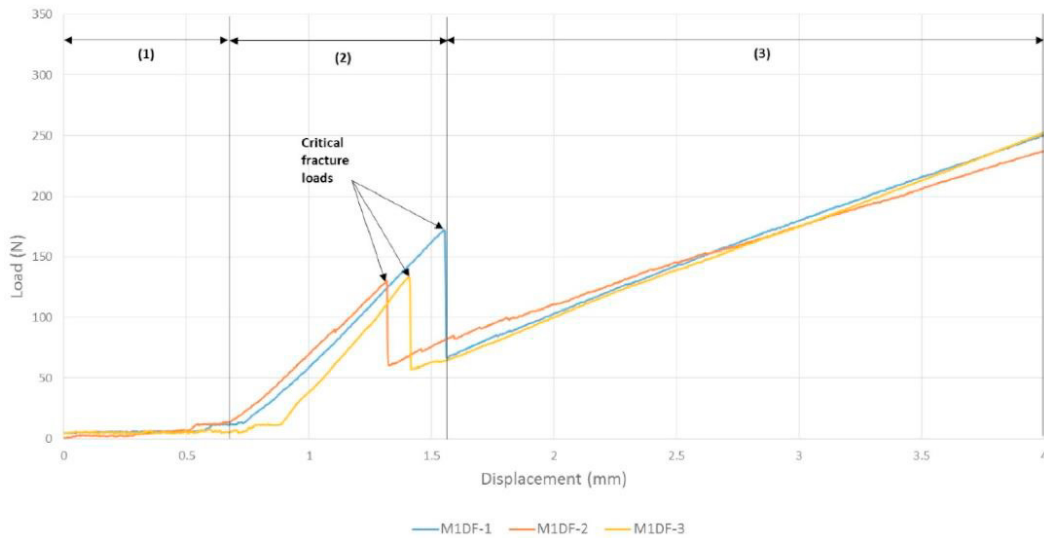


Fig. 3. Load displacement profiles for mixed mode testing with different loading zones.

Figure 4 shows the average AE energy recorded during the entire test period along with loading profiles. For all specimens tested, AE energy showed a steady increase towards adhesive failure. This was conveyed as a large spike, prominent in every plot which coincided with the critical loading point. A good degree of repeatability was exhibited throughout the testing and particular by the (M1.D.100) samples, where all features were found to align accurately. Larger energy signals were observed beyond the critical loading, with greater fluctuation as time and loading increased when compared to brittle adhesive. It should be noted here that the higher consistency achieved for ductile adhesive specimens is due to the difference in curing behaviour of the adhesive types where the brittle adhesive required less curing time than ductile and was prone to sliding, and hence, less uniform contact between both substrates. This would have contributed to the great variation in AE energy between the brittle specimens. Typically, very low AE energy was recorded during the linear elastic deformation of the adhesive layer, which is consistent with studies conducted by Droubi et al. (2017). However, the 65% bonded specimens exhibited greater AE energy activity around the initial peak value and often presented energy readings prior to the critical load point which was attributed to inconsistencies in bond quality between each specimen due to manual application of PTFE spray.

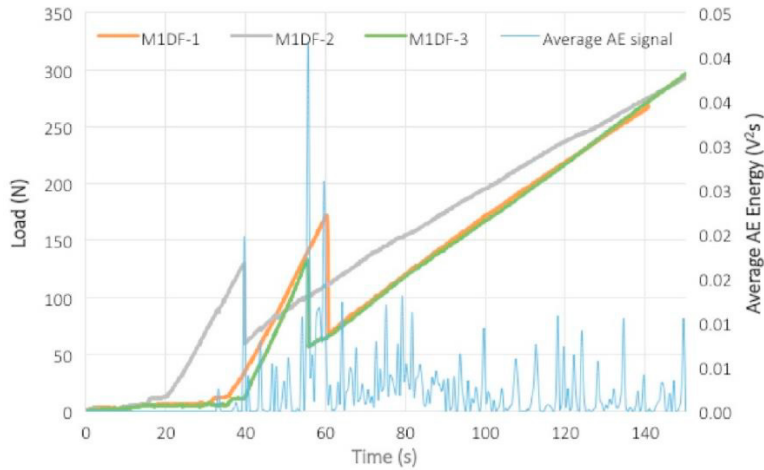


Fig. 4. Average AE energy and loading graphs for the specimen (M1.D.100).

Figure 5 demonstrates a measure of the specimens' fracture toughness's under mixed-mode loading conditions. As can be seen, a higher fracture toughness under mixed-mode 2 (M2), where a greater proportion of mode II fracture energy was produced, was obtained for all tested specimens. The greatest value of  $G_c$  under mixed-mode 1 (M1) was found to be 25.689 J/m<sup>2</sup>, for the 'fully' bonded specimen with ductile adhesive (M1.DF). This was 62% lower than the highest value of  $G_c$  under mixed-mode 2 (67.830 J/m<sup>2</sup>). This was observed in the fully bonded specimen with brittle adhesive (M2.B.100). The M1 configuration, with a higher proportion of mode I fracture energy, resulted in a wider range of fracture points implying a longer crack length at the point of adhesive failure in the specimen (Senthil et al. 2016). This ranged from 45 mm to 62 mm, compared with crack lengths between 48 mm to 54 mm for M2. This highlighted more unstable crack propagation under mixed-mode M1 than mixed-mode M2.

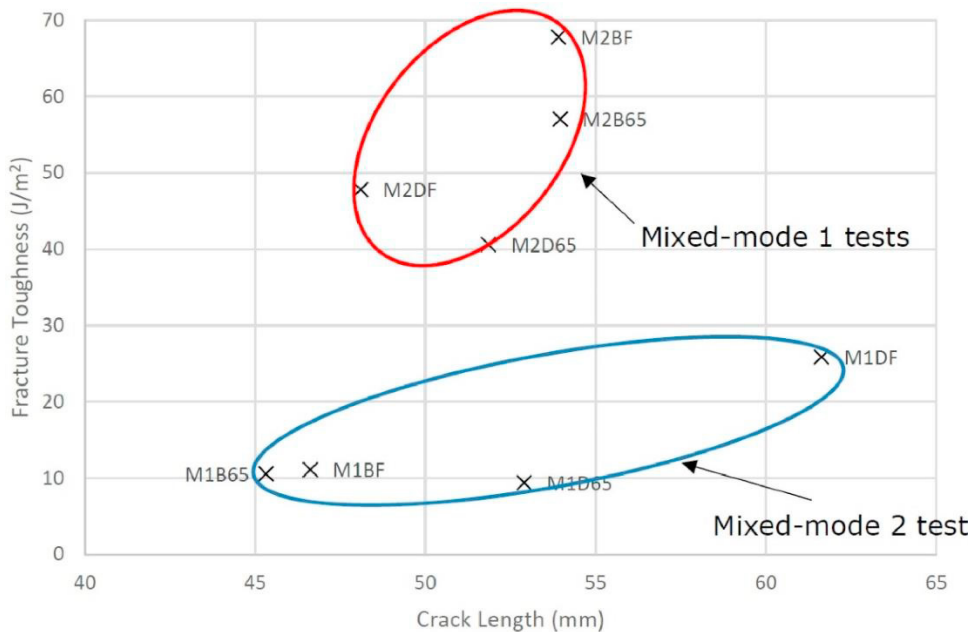


Fig. 5. Fracture toughness of specimens.

Another trend in the results was the higher fracture toughness of the fully bonded specimens compared to the 65% partially bonded ones. This was the expected outcome before testing, as the percentage of bonded area directly relates to the strength of the adhesive bond. This was true for all specimen configurations. The smallest difference between the fully and partially bonded was observed in the brittle adhesive specimens under M1 (1.7%) and the greatest difference was observed in the ductile adhesive specimens under M1 (63.4%). Except for one specimen (M1.B.100), it was found (Table 2) that specimens bonded with brittle adhesive showed greater fracture toughness than those bonded with ductile adhesive. It is difficult to make the claim that the brittle adhesive performed better due to not all results conforming to this trend; however, the rest of the data is indicative of this.

Table 2. Full set of results.

Specimen	Critical Load (N)	Critical G (J/m <sup>2</sup> )	Specimen	Critical Load (N)	Critical G (J/m <sup>2</sup> )
M1.D.65	145.10	9.412	M2.D.65	261.72	42.97
M1.D.100	172.02	25.69	M2.D.100	296.60	47.82
M1.B.65	147.65	10.92	M2.B.65	290.60	57.04
M1.B.100	149.79	11.11	M2.B.100	317.19	67.83

### 3.2. Finite element analysis of mixed mode bending

Finite element modelling results were validated using an inverse method to match the load vs. displacement graph with that of specimen (M2.D.100). The finite element analysis allowed for the effect of varying different parameters to be investigated that were not varied in the experimental procedure. Figure 6 shows the loading profiles for four variant models of different adherend thicknesses alongside the original model with 6 mm adherends. As can be seen, increasing the adherend thickness would result in a steady increase in the critical load value. Similarly, the effect of varying the pre-crack length was investigated and the results showed that an increase in the pre-crack length resulted in a lower magnitude of force required before the adhesive bond failed. As the initial crack length was increased, the more detrimental it was on the performance of the adhesive joints, shown by the drop off in critical load values as the length was increased.

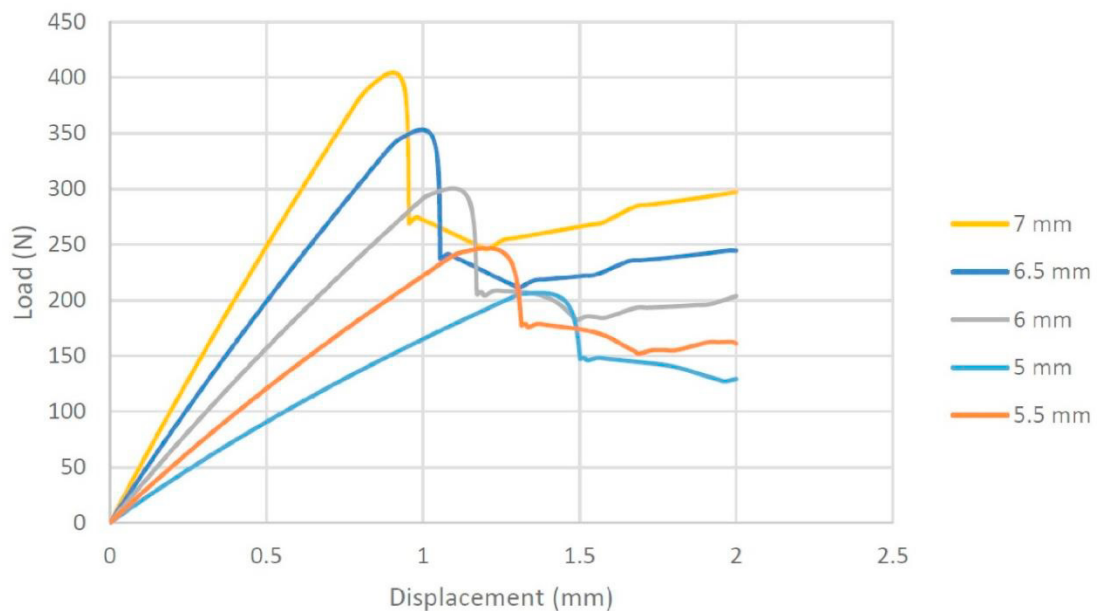


Fig. 6. Loading profiles for different adherend thicknesses.

#### 4. Conclusions

In this study, the mixed-mode (I+II) fracture behaviors of adhesively bonded joints were analysed and tested under different test conditions. The specimens were tested under two different mixed-mode ratios, with either a higher proportion of mode I or mode II loading, and with varied bond qualities with the following conclusion:

- The AE analysis was correlated well with adhesive failure where a distinct significant AE event was identified for all testes specimens which may serve as a useful technique for monitoring the failure of adhesively bonded joints.
- Specimens tested under a mixed-mode ratio of 2:1 for  $G_I/G_{II}$  fractured at a loading 48% lower on average than those under a ratio of 1:2. This demonstrated the adhesive bond's greater resistance to mode II shearing forces and highlighted the importance of mitigating mode I opening forces in structures subjected to mixed-mode loading conditions.
- The numerical study gave an insight into the effects of varying test parameters that would not have been feasible to change experimentally, considering practical constraints. Increasing the adherend thickness was found to increase the critical load value while increasing the pre-crack length was found to reduce the force required before the adhesive bond failed.

#### References

- ASTM D6671 / D6671M-13e1, Standard test method for mixed mode I-mode II interlaminar fracture toughness of unidirectional fiber reinforced polymer matrix composites, ASTM International, West Conshohocken, PA, 2013, [www.astm.org](http://www.astm.org)
- Choupani, N., 2008. Mixed-mode cohesive fracture of adhesive joints: Experimental and numerical studies. *Engineering Fracture Mechanics* 75, 4363-4382.
- Davis, M.J., McGregor, A., 2010. Assessing adhesive bond failures: mixed-mode bond failures explained. ISASI Australian Safety Seminar, Canberra, The International Society of Air Safety Investigators (ISASI), 04.06–06.06.
- Droubi, M.G., Stuart, A., Mowat, J., Noble, C., Prathuru, A.K., Faisal, N.H., 2017. Acoustic emission method to study fracture (Mode-I, II) and residual strength characteristics in composite-to-metal and metal-to-metal adhesively bonded joints. *The Journal of Adhesion* 1-40.
- Dzenis, Y.A., Saunders, I., 2002. On the possibility of discrimination of mixed mode fatigue fracture mechanisms in adhesive composite joints by advanced acoustic emission analysis. *International Journal of Fracture* 117, 23–28.
- Prathuru, A.K., Faisal, N.H., Jihan, S., Steel, J.A., Njuguna, J., 2016. Stress analysis at the interface of metal-to-metal adhesively bonded joints subjected to 4-point bending: Finite element method. *The Journal of Adhesion*. 12, 1–24.
- Sachse, W., Kim, K.Y., 1987. Quantitative acoustic emission and failure mechanics of composite materials. *Ultrasonics* 25, 195-203.
- Senthil, K., Palaninathan, R., Arockiarajan, A., 2016. Experimental determination of fracture toughness for adhesively bonded composite joints. *Engineering Fracture Mechanics* 154, 24-42.
- Vine, K.A., 1999. The non-destructive testing of adhesive joints for environmental degradation, PhD thesis. Imperial College of Science Technology and Medicine, University of London, 22-26.